JOURNAL OF MATERIALS SCIENCE 32 (1997) 6215–6220

The effect of heat treatment on the tensile and creep behaviour of "neat" matrix Ti–22Al–23Nb

P. R. SMITH
Materials Directorate, Wright Laboratory, Wright-Patterson Air Force Base, OH 45433, USA
W. J. PORTER
University of Dayton Research Institute, Dayton, OH 45469, USA

A study has been conducted to examine the effect of post-consolidation heat treatment on the longitudinal tensile and creep properties of an orthorhombic-based titanium aluminide, Ti–22Al–23Nb (a %), in neat matrix form. Heat-treatment parameters were selected such that they would be consistent with future inclusion into the consolidation cycle for the fabrication of continuously reinforced orthorhombic titanium matrix composites (O TMCs). The effects of heat treatment on microstructural evolution, including type and morphology of the phase constituents, was examined via scanning secondary electron microscopy and quantitative image analysis. Variations in microstructural features were correlated with resulting room-temperature tensile properties including: ultimate tensile strength, yield strength, total elongation and modulus, as well as isothermal creep response at 650 °C/172 MPa.

1. Introduction

Titanium aluminide composites based upon Ti_3Al (alpha-2, hexagonal DO_{19} structure) have been the subject of numerous investigations in recent years [1, 2]. The majority of these studies have focused on a SiC-reinforced Ti24Al–11Nb (at %) matrix alloy as representative of this class of materials. The deficiencies associated with this alloy as a matrix for compositing have been well documented, and include poor fibre matrix reactivity, modest low- and elevated-temperature tensile strength, low fracture resistance, poor creep response and high sensitivity to interstitial embrittlement [3, 4]. Recent studies have begun to focus on an alternative titanium aluminide matrix alloy based upon the Ti_2AlNb (orthorhombic) phase [5]. Results from studies involving the orthorhombic composition, Ti–22Al–23Nb (at %) [6, 7] seem to suggest that this matrix class offers the following benefits relative to Ti–24Al–11Nb: reduced fibre matrix reactivity, improved fracture resistance, increased tensile strength and increased resistance to elevated temperature creep deformation. Unfortunately, the creep response obtained even for the Ti–22Al–23Nb alloy in its as-fabricated form, still falls short of the required 100 h to 0.4% creep strain goal established for advanced propulsion applications currently under consideration. Therefore, the objective of the subject study was to utilize a post-consolidation heat treatment as a means to modify the matrix microstructure of the Ti–22Al–23Nb alloy, in order to improve its tensile and creep performance.

2. Experimental procedure

The neat Ti–22Al–23Nb matrix material utilized in the subject study was produced using a conventional ingot to foil reduction approach. Atlantic Research/IMT fabricated the neat matrix material by hot isostatic pressing (HIPing) five foils laid up in the same orientation with respect to the foil rolling direction. Longitudinally oriented rectangular specimens measuring 10 mm (w) × 100 mm (l) × 0.1 mm (t) were machined from the neat panels using low-speed diamond cutting. Specimens were wrapped in tantalum and heat treated in vacuum (10^{-6} torr; 1 torr = 133.322 Pa) after flushing with high-purity argon.

All heat treatments were applied after consolidation of the neat matrix. All of the solution heat-treatment temperatures investigated were higher than the consolidation temperature. The beta transus of Ti–22Al–23Nb neat material was determined to be approximately 1100 °C, using the disappearing phase technique. A total of four solution heat-treatment temperatures were examined: three sub-transus (1025, 1050 and 1075 °C) and one super-transus (1125 °C). In addition, two cooling rates (direct from the solution heat-treatment temperature to the ageing temperature) were evaluated: 28 and 2.8 °C min^{-1}. The slower cooling rate was selected to be commensurate with those encountered during composite consolidation. Finally, three ageing schemes were studied: 760 °C/16 h, 815 °C/8 h and 870 °C/4h. The baseline heat treatment selected for the study was

0022–2461

1075 °C/2 h + 28 °C min^{-1} + 815 °C/8 h/furnace cooled (FC). The heat-treatment conditions were selected such that they could be integrated into the composite fabrication cycle.

Microstructural analysis including determination of phase distribution, morphology and size was accomplished by secondary imaging of the as-fabricated and heat-treated neat materials using a Leica 360FE scanning electron microscope (SEM) with a spatial resolution of 2 nm at 25 kV. Volume fraction determination of the constituent phases was accomplished using an image analysis program via a density slice function applied to stored digital back-scattered SEM images. Microstructural characteristics were correlated with corresponding mechanical property levels.

Mechanical behaviour examination included room-temperature (23 °C) tensile properties, as well as elevated-temperature isothermal creep (650 °C/172 MPa). A minimum of two tensile tests were conducted per heat-treatment condition. Tensile tests were conducted under stroke-control at a constant crosshead speed of 0.0084 mm s^{-1}. Two creep tests were run per condition: (1) to 0.4% creep strain, and (2) to at least 300 h creep life. All tests were conducted on a horizontal servo-hydraulic system. Details regarding the test system can be found elsewhere [8].

3. Results and discussion

3.1. Microstructure

The as-fabricated neat microstructure is displayed in Fig. 1. It is seen to contain three ordered phases, consistent with previous results for orthorhombic alloys of similar chemistry containing high levels of oxygen [9]. The dark primary phase is alpha-2 (α_2) or Ti_3Al (hexagonal DO_{19} structure). This phase represents approximately 35 vol % of the structure, is fine-grained (5–10 μm) and relatively equiaxed. The two-phase mixture is a combination of orthorhombic "O" (light grey) platelets (~ 1 μm × 5 μm) in an ordered beta (B2) matrix (white). The "O" phase is based upon the Ti_2AlNb composition and represents a distortion of the α_2 structure by changing slightly the magnitude of the Burger's vectors of equivalent a and $c + a$ dislocations in the α_2 structure. Note, Graves *et al.* [10] had previously determined that the beta phase was ordered for this composition. In addition, the perimeter of primary α_2 phase is encased by a thin layer (~ 0.5 μm) of "O" phase; however, it has not been determined if this is the same variant as the "O" platelets formed from the B2 phase. Previous studies [5] have indicated that the "O" phase can form a transformation product from the B2 phase after solution treatment during ageing, or by a phase separation reaction within the α_2 phase (i.e. niobium segregates to the perimeter of the α_2). The corresponding volume fractions of the "O" and B2 phases were found to be 34 and 31 vol %, respectively, with the B2 phase being continuous.

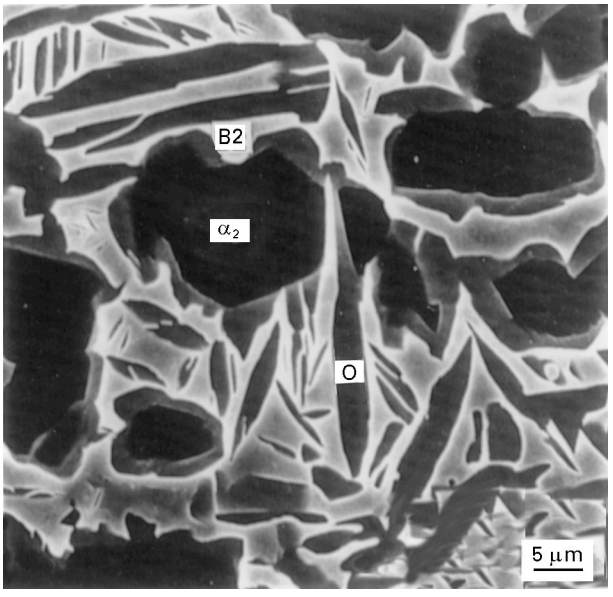

Figure 1 As-fabricated neat microstructure containing three ordered phases: O, B2 and α_2.

The scanning electron micrographs in Fig. 2 show the effects of solution heat treatment on microstructural response. In this instance, the cooling rate and ageing treatment conditions were held constant at 28 °C min^{-1} and 815 °C/8 h/FC, respectively. It can be seen that the primary α_2 phase content decreases continually up through the 1075 °C solution treatment, after which it is totally dissolved as the beta transus is exceeded at 1125 °C. An inverse relationship was found for the "O" phase content in that it is seen to be continually increasing with increasing solution-treatment temperature. The B2 phase content appears to be relatively unchanged, and thus, the increase in "O" appears to be associated with a corresponding decrease in α_2. Previous studies [11] have indicated that the α_2 phase has poor ductility below ~ 600 °C owing to the anisotropy of slip associated with the DO_{19} structure. $\langle a \rangle$ Slip is seen to occur relatively easily on the prism plane, while $\langle c + a/2 \rangle$ slip is very difficult. As a result, large incompatibility stresses can build up at α_2/α_2 interfaces. As the solution heat-treatment temperature increases, the number of α_2/α_2 interfaces decreases, and the surrounding B2 phase acts to accommodate these stresses. In addition, Koss *et al.* [11] demonstrated that the amount of $c + a$ slip available for the "O" phase is significantly more than for the α_2 phase.

3.2. Tensile behaviour

Table I contains the tensile properties corresponding to the solution heat-treatment conditions previously discussed. In almost all instances the ultimate tensile strength (UTS), yield strength (YS), percentage elongation (% El) and modulus, E, have increased relative to the as-fabricated condition. The only exception to this being the ductility (elastic + plastic) after the 1125 °C solution treatment. The 1050 °C solution treatment appears to provide the best combination of UTS, %El and modulus. It would appear that the increase in tensile properties is associated with an increase in the volume fraction of the lenticular "O" phase and a corresponding decrease in the equiaxed α_2 phase.

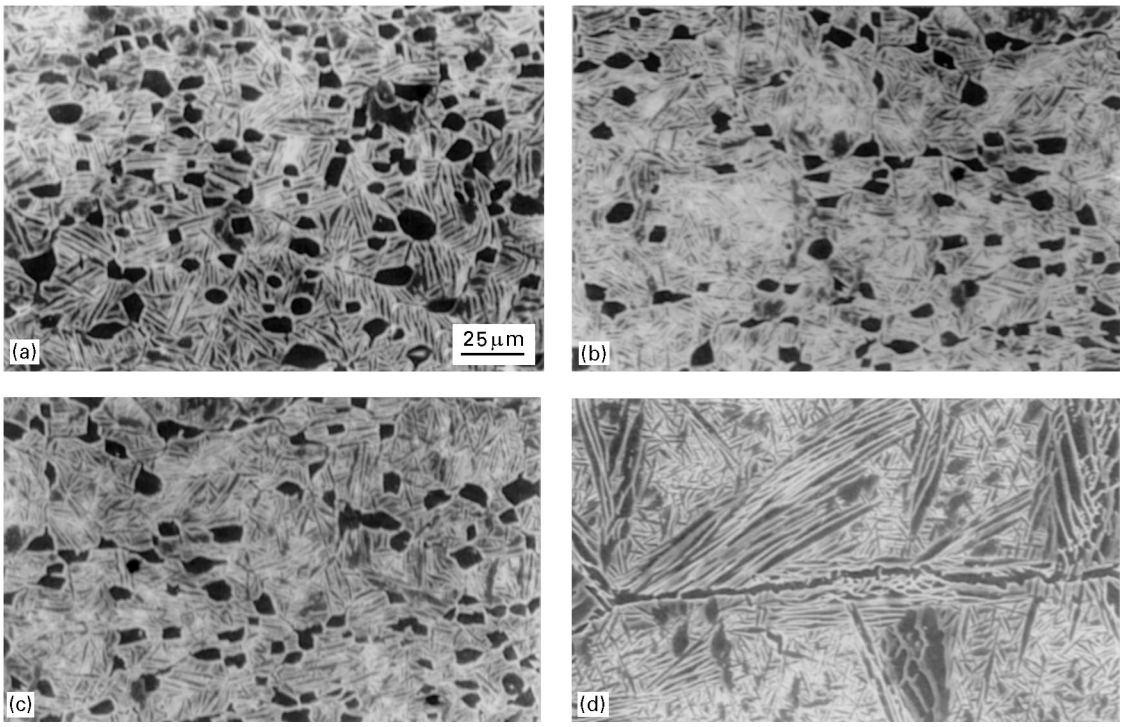

Figure 2 Effect of solution heat-treatment temperature on microstructure (cooling rate = 28 °C min^{-1}; age = 815 °C/8 h/FC): (a) 1025 °C, (b) 1050 °C, (c) 1075 °C, (d) 1125 °C.

TABLE I Effect of solution heat-treatment on tensile properties

Condition	UTS (MPa)	YS (MPa)	%El	Modulus (GPa)
As-fabricated	972	805	8.4	105
1025 °C/2 h[a]	1096	848	9.0	119
1050 °C/2 h[a]	1111	836	14.8	121
1075 °C/2 h[a]	1059	810	11.5	120
1125 °C/2 h[a]	1053	926	4.0	135

[a] Solution heat treatment + 28 °C min^{-1} + 815 °C/8 h/FC.

TABLE II Effect of cooling rate and ageing treatment on tensile behaviour

Condition	UTS (MPa)	YS (MPa)	%El	Modulus (GPa)
As-fabricated	972	805	8.4	105
Baseline HT[a]	1059	810	11.5	120
2.8 °C min[b]	946	725	11.2	114
760 °C/16 h/FC[c]	1098	931	5.5	109
870 °C/4 h/FC[c]	1062	810	12.3	113

[a] 1075 °C/2 h + 28 °C min^{-1} to 815 °C/8 h/FC.
[b] Solution HT = 1075 °C/2 h; age = 815 °C/8 h/FC.
[c] Solution HT = 1075 °C/2 h; cooling rate = 28 °C min^{-1}.

Having determined the effect of solution heat-treatment temperature on tensile properties, the effects of cooling rate and ageing treatment were independently examined. First, the effect of reducing the cooling rate by a factor of 10 from 28 °C min^{-1} to 2.8 °C min^{-1} was evaluated by selecting a constant solution heat treatment of 1075 °C/2 h and a constant ageing treatment of 815 °C/8 h/FC. The results are contrasted (Table II) with the as-fabricated condition, and the baseline heat treatment, where in the latter the cooling rate was 28 °C min^{-1}. It can be noticed that the UTS and YS both drop with respect to both the as-fabricated and baseline conditions, that the ductility is similar to the baseline heat treatment, and the modulus is intermediate to the two conditions. The decrease in strength is most likely associated with increased lath size of the "O" platelets and hence the mean free slip length across individual platelets. Previous studies by Pank *et al.* [12] suggest that strength is inversely proportional to this mean slip length. In addition, the volume fraction of the lower strength α_2 phase has increased.

In a similar fashion, the effect of ageing treatment was evaluated by again holding the solution-treatment condition (1075 °C/2 h) and cooling rate (28 °C min^{-1}) constant, while examining two additional (beyond the baseline 815 °C/8 h) ageing treatments of 760 °C/16 h and 870 °C/4 h. The results of the two ageing treatments on tensile properties are also shown in Table II. The lower temperature age provides for a slight increase in UTS, and a relatively large increase in YS when compared to the as-fabricated and baseline heat-treatment conditions. In addition, a significant decrease in ductility and an intermediate modulus value can be observed. These changes can be explained in terms of the resulting microstructure. It was noticed that the lower ageing temperature resulted in a much finer O + B2 secondary structure, as well as, a semi-continuous layer of α_2. The finer scale of the secondary structure gives rise to increased strength levels due to Hall–Petch boundary strengthening, while conjunction with the semicontinuous nature of the α_2, results in reduced ductility for reasons noted earlier. The higher temperature ageing treatment results in UTS, YS and %El values similar to that of the baseline heat-treatment

condition with an intermediate modulus value. It was observed that the resulting microstructure had changed relative to the 815 °C age, in that the volume fraction of α_2 increased, but it remained discontinuous. In addition, the "O" lath size had increased, while the B2 phase remained continuous. The fracture morphology of the 760 °C age was dominated by transgranular cleavage of both the "O" platelets and α_2 grains with little evidence of ductile dimpling. Conversely, the material when aged at 870 °C displayed a fracture exhibiting a significant amount of ductile dimpling produced by microvoid coalescence of, primarily, the B2 phase, while transgranular fracture of the α_2 and "O" phases was still observed.

The overall results of the effect of heat treatment on tensile behaviour would seem to suggest that the Ti–22Al–23Nb alloy is heat treatable to improved combinations of UTS, YS, %El and modulus compared to the as-fabricated neat matrix. Furthermore, if a combination of good strength and ductility are required, a heat treatment incorporating a high subtransus ($\beta_{tr} - 50$ °C) solution treatment followed by a rapid cool (28 °C min^{-1}) and intermediate to high temperature (815–870 °C) ageing provide the best results.

3.3. Creep behaviour

The effects of solution heat treatment on isothermal creep behaviour at 650 °C/172 MPa are shown in Table III. As previously noted, two tests per condition were run: (1) to 0.4% total creep strain, and (2) to 300 h creep life. Therefore, the times shown to 0.4% creep strain are the average of two data points, while the 300 h rupture criterion represents a singular value. Also shown are the minimum creep rates and the time spent in the primary transient creep regime as determined by the inflection of the creep curve to steady-state conditions. It can be noticed as the solution heat-treatment temperature increases, the time to 0.4% creep strain increases such that the super-transus treatment provides for an increase of $> 15\times$ life extension compared to that for the as-fabricated condition. In addition, each of the solution treatments results in a rupture life which exceeds the 300 h criterion. The super-transus excursion also results in approximately an order of magnitude increase in the minimum creep rate. Finally, all of the solution treatments result in a significant extension of the primary transient creep regime.

In an effort to understand the effect of microstructure on damage accumulation during creep, a neat sample which had been solution treated and directly aged (1025 °C/2 h + 28 °C min^{-1} + 815 °C/8 h/FC) was crept at 650 °C/172 MPa to a total creep strain of $\sim 2.0\%$. The corresponding microstructure is shown in Fig. 3. It can be noticed (Fig. 3a) that the primary deformation mode appears to be by crack initiation at the interface between the "O" phase (at the rim of the primary α_2 and adjacent phase(s). Furthermore, there

TABLE III Effect of solution treatment temperature on 650 °C/172 MPa isothermal creep

Condition	Time (h)			300 h	S.S. creep rate ($\times 10^{-8}$)	Primary creep (h)
	0.2%	0.4%	1.0%			
As-fabricated	1.4	5.4	28	No (147 h)	3.1	57
1025 °C	3.0	12.4	63	Yes	1.6	180
1050 °C	8.7	31.1	179	Yes	1.2	200
1075 °C	8.5	41.0	290	Yes	1.2	220
1125 °C	22.5	87.5	[a]	Yes	0.59	225

[a] Did not reach 1.0% creep strain before 300 h criterion was met.

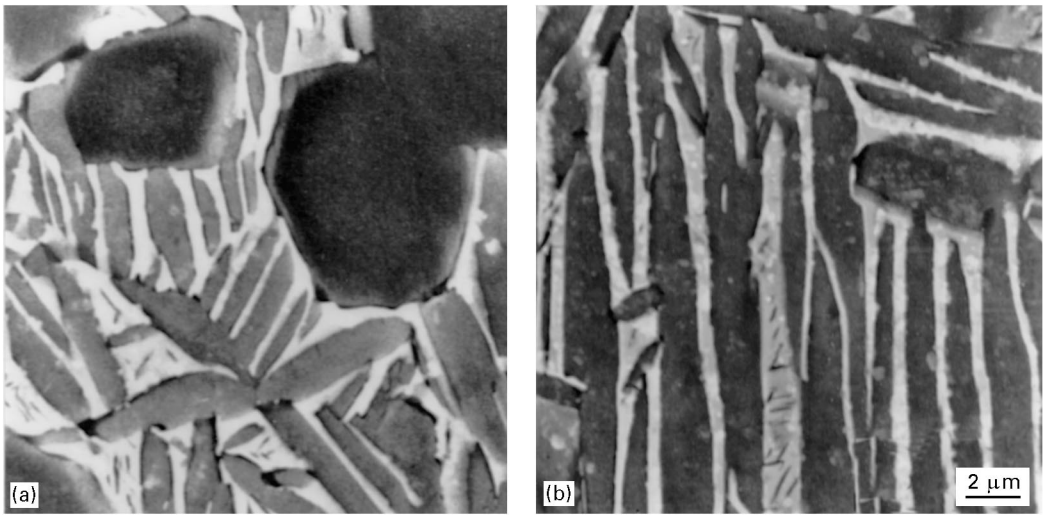

Figure 3 Creep damage accumulation at 650 °C/172 MPa to 2.0% creep strain indicating (a) crack initiation at interface of rim "O" and adjacent phases, and (b) no cracking at lath "O"/B2 interfaces.

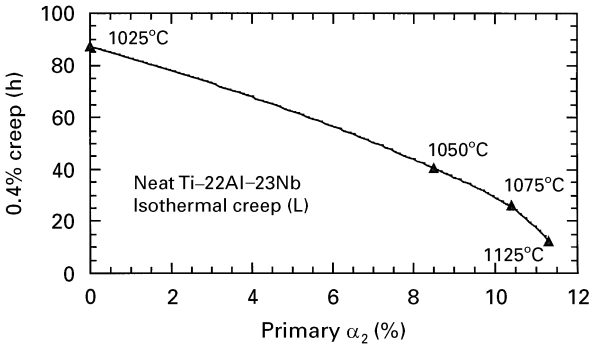

Figure 4 Effect of volume fraction of primary α_2 phase on time required to reach 0.4% creep strain at 650 °C/172 MPa.

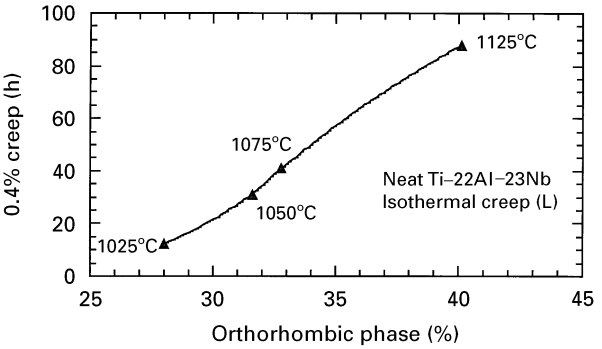

Figure 5 Effect of volume fraction of "O" phase on time to reach 0.4% creep strain at 650 °C/172 MPa.

is little evidence of crack initiation at the lath "O"/B2 interfaces (Fig. 3b). Therefore, one might deduce that if the volume fraction of the primary equiaxed α_2 phase was decreased (and hence the volume fraction of the rim "O" phase), and correspondingly, the volume fraction of the lath "O" phase was increased, that the creep resistance would increase. Fig. 4 contains a plot of the time required to reach a creep strain of 0.4% versus the volume fraction of primary α_2 present in the microstructure. It is seen that as the volume fraction of primary α_2 decreases, the time to reach 0.4% creep strain steadily increases. Conversely, Fig. 5 illustrates the effect of lath "O" phase content on time required to reach 0.4% creep strain. Here it is seen, that as the volume fraction of lath "O" phase increases, so does the creep resistance. It should be noted that in both instances, the volume fraction of B2 remains essentially constant, such that the increase in lath "O" is proportional to the decrease in equiaxed α_2. There at at least two possible explanations for this behaviour. First, it has been previously demonstrated for $\alpha_2 + \beta$ alloys, Ti–25Al–10Nb–3V–1Mo and Ti–24Al–11Nb, that lath structures are stronger in creep than equiaxed structures [13–15]. Furthermore, Banerjee *et al.* [16] have demonstrated that the "O" phase is substantially stronger in creep resistance than the α_2 phase.

The effect of ageing treatment and cooling rate on the creep response of neat Ti–22Al–23Nb is depicted in Table IV. Comparisons are made against the as-fabricated condition and the baseline heat-treatment condition (1075 °C/2 h + 28 °C min^{-1} + 815 °C/8 h/FC). It can be seen that all of the heat treatments resulted in improved creep resistance when compared to the as-fabricated condition. This is most likely the result of increased levels of "O" phase and lath microstructure and corresponding decreases in equiaxed α_2. It can be noticed that the effect of ageing treatment on creep response was rather minimal. Both the high- and low-temperature ageing temperatures resulted in very similar times to 0.4% creep strain, steady-state creep rates, and primary transient creep lives. This was true despite the fact that the volume fractions of the various phases were changing, as well as the scale of the lath microstructure. This observation can be explained in terms of competing effects. The low-temperature ageing treatment resulted in a much finer lath size which would tend to favour increased creep rates. However, the same ageing treatment produced decreased levels of α_2 with corresponding increases in lath "O", both of which tend to result in decreased creep rates. Similarly, for the high-temperature age, the scale of the lath structure has increased, while the volume fraction of α_2 increases and the "O" phase decreases. The net result is that the creep performance remains essentially unchanged when compared to the baseline ageing condition. The effect of cooling rate was more dramatic. It is noticed that reducing the cooling rate by an order of magnitude to 2.8 °C min^{-1} results in a two-fold decrease in the time to 0.4% creep strain, although the steady state creep rate and primary transient creep life remain essentially unchanged. This result can be rationalized by noting that the slower cooling rate produced a lath structure similar in width to that observed for the faster cooling rate, but reduced in length, while the

TABLE IV Effect of ageing treatment and cooling rate on 650 °C/172 MPa isothermal creep

Condition	Time (h)			300 h Rupture Criterion?	S.S. creep rate ($\times 10^{-9}$)	Primary life (h)
	0.2%	0.4%	1.0%			
As-fabricated	1.4	5.4	28	No (147 h)	3.1	57
Baseline	8.5	41.0	290	Yes	1.2	220
Low temp age[a]	9.4	36.8	214	Yes	6.8	230
High temp age[b]	6.9	36.8	226	Yes	8.2	240
Slow cool rate[c]	3.8	19.6	129	Yes	9.0	230

[a] 1075 °C/2 h + 28 °C min^{-1} + 760 °C/16 h/FC.
[b] 1075 °C/2 h + 28 °C min^{-1} + 870 °C/4 h/FC.
[c] 1075 °C/2 h + 28 °C min^{-1} + 815 °C/8 h/FC.

relative volume fractions of α_2 increased and "O" decreased.

4. Conclusion

This study has demonstrated the effects of post-consolidation heat treatments on the longitudinal tensile and creep performance of a neat "orthorhombic" titanium aluminide composition, Ti–22Al–23Nb (at %). The heat treatments were chosen such that they might eventually be incorporated into the consolidation cycle for continuous fibre-reinforced composites. It was found that this composition, much like conventional $\alpha + \beta$ titanium alloys, can be heat treated to improved combinations of tensile and creep performance.

All of the sub-transus heat treatments resulted in an increase in UTS, YS, %El and modulus with respect to the as-fabricated condition, with the exception of the slower cooling rate which had slightly inferior UTS and YS values. The best balance of properties was produced by the β_{tr}–50 °C (i.e. 1050 °C) solution treatment. These increases were rationalized in terms of increases in lath "O" phase content, decreases in equiaxed α_2, and refinement in microstructural features. A super-transus solution treatment resulted in significant improvements in UTS, YS and modulus, again compared to the as-fabricated condition, but with reduced ductility as a result of aligned α_2 or "O" platelet formation at or near prior beta grain boundaries. The isothermal creep performance (650 °C/172 MPa) provided by each of the heat treatments, was also improved compared with the as-fabricated condition. The effect of solution treatment on time to reach 0.4% creep strain was correlated with volume fractions of equiaxed α_2 and lath "O". It was found that increases in lath "O" and associated decreases in equiaxed α_2, increased creep performance. The best creep results were afforded by the super-transus solution treatment, $\beta_{tr} + 25$ °C (i.e. 1125 °C), which provided for a 15× life extension to 0.4% creep strain. The effect of ageing temperature on creep was found to be minimal over the range of temperatures examined (760–870 °C). This was rationalized based upon competing effects of relative volume fractions of phases and "O" lath size. The effect of decreasing the cooling rate (between solution treatment and ageing temperatures) by an order of magnitude, reduced the time to 0.4% creep strain by a factor of ~ 2, as a result of increased equiaxed α_2 and decreased lath "O" volume fractions. While all of the heat treatments surpassed a 300 h rupture criterion, none exceeded the 100 h to 0.4% creep strain requirement (although the super-transus solution treatment resulted in > 87 h). This would suggest that alloy modification in combination with heat treatment may be required. In addition, the effects of the subject heat treatments on transverse properties, as well as cyclic response, are the focus of continuing studies. Finally, optimum heat treatment(s) must be applied to the fibre-reinforced composite and evaluated for their effect on composite mechanical performance.

Acknowledgements

The authors gratefully acknowledge the contributions of Mr Dan Knapke and Ms Debra Garner, University of Dayton Research Institute, for mechanical testing performed under AF Contract F33615-91-C-5606, as well as Mr Mark Dodd for heat treatment and Mr Eric Fletcher for specimen preparation, all of Universal Energy Systems working under AF Contract 33615-93-C-5663.

References

1. J. M. LARSEN, W. C. REVELOS and M. L. GAMBONE, "in Intermetallic Matrix Composites II", edited by D. B. Miracle, D. L. Anton and J. A. Graves (Materials Research Society, Pittsburgh, PA, 1992) p. 3.
2. R. A. MACKAY, P. K. BRINDLEY and F. H. FROES, *JOM* **43** (5) (1991) 23.
3. P. R. SMITH and W. C. REVELOS, in "Fatigue '90", edited by H. Kitagawa and T. Tanaka (MCE Publications, Birmingham, UK, 1990) p. 1711.
4. W. C. REVELOS and P. R. SMITH, *Metall. Trans. A* **23** (1992) 587.
5. D. BANERJEE, A. K. GOGIA, T. K. NANDY and V. A. JOSHI, *Acta Metall.* **36** (1988) 871.
6. P. R. SMITH, J. A. GRAVES and C. G. RHODES, in "Intermetallic Matrix Composites II", edited by D. B. Miracle, D. L. Anton and J. A. Graves (Materials Research Society, Pittsburgh, PA, 1992) p. 43.
7. P. R. SMITH, J. A. GRAVES and C. G. RHODES, *Metall. Trans. A* **25** (1994) 1267.
8. G. A. HARTMAN and S. M. RUSS, in "Metal Matrix Composites: Testing, Analysis and Failure Modes", edited by W. S. Johnson (American Society for Testing and Materials, Philadelphia, PA, 1989) p. 43.
9. C. G. RHODES, J. A. GRAVES, P. R. SMITH and M. R. JAMES, in "Structural Intermetallics", edited by R. Darolia, J. J. Lewandowski, C. T. Liu, P. L. Martin, D. B. Miracle and M. V. Nathal, (TMS-AIME, Warrendale, PA, 1993) p. 45.
10. J. A. GRAVES, P. R. SMITH and C. G. RHODES, in "Intermetallic Matrix Composites II", edited by D. B. Miracle, D. L. Anton and D. L. Graves, (Materials Research Society, Pittsburgh, PA, 1992) p. 31.
11. D. A. KOSS, D. BANERJEE, D. A. LUKASAK and A. K. GOGIA, in "High Temperature Titanium Aluminides and Intermetallics", edited by S. H. Whang, C. T. Liu, D. P. Pope and J. O. Stiegler (TMS-AIME, Warrendale, PA, 1990) p. 175.
12. D. R. PANK, A. M. RITTER, R. A. AMATO and J. J. JACKSON in "Titanium Aluminide Composites", Report WL-TR-91-4020, edited by P. R. Smith, S. J. Balsone and T. Nicholas, Materials Directorate, Wright Laboratory, Wright-Patterson AFB (1991) p. 38.
13. D. E. ALBERT and A. W. THOMPSON, *Metall. Trans. A* **23** (1992) 3035.
14. W. CHO, A. W. THOMPSON and J. C. WILLIAMS, *ibid.* **21** (1990) 641.
15. R. W. HAYES, *Acta. Metall.* **39** (1991) 569.
16. D. BANERJEE, A. K. GOGIA, T. K. NANDY, K. MURALEEDHARAN and M. S. MISHRA in "Structural Intermetallics", edited by R. Darolia, J. J. Lewandowski, C. T. Liu, P. L. Martin, D. B. Miracle and M. V. Nathal, (TMS-AIME, Warrendale, PA, 1993) p. 19.

Received 27 February
and accepted 29 May 1997